Subtle MR Guidance for Partial Volume Correction of PET Images: A Comparison of Techniques

Yansong Zhu, Yuanyuan Gao, and Arman Rahmim

Abstract*—Quantitative accuracy of PET is influenced by the partial volume effect. Different MR-based partial volume correction (PVC) methods have been proposed to tackle this issue. Early methods like geometric-transfer matrix (GTM) require segmentation of MR images into different regions and also make the strong assumption that activity distribution in each region is constant. Though they have shown good performance with perfect MR guidance, imperfect MR information may degrade their performance. Our hypothesis is methods that make subtle usage of MRI images can prove more advantageous and depict greater feasibility and strength for translation to routine usage. In this work, we compared different MR-guided post-reconstruction PVC methods with perfect and imperfect MR guidance due to errors in registration and segmentation. We considered PVC methods that perform subtle MR guidance, including our two recently proposed methods: anatomical-guided non-local mean (NLMA) and split Bregman based parallel level set (SBPLS), which solves PLS with non-smooth optimization technique and shows advantages compared to ordinary smooth optimization framework, as well as symmetric (sBowsher) and asymmetric Bowsher (aBowsher), and PLS solved with smooth optimization technique. Region-based voxel-wise (RBV) method, a GTM-based method, was also taken for comparison. Reblurred Van Citter (VC) deconvolution method was chosen as a reference method that does not use MR information at all. These methods were evaluated with realistic simulation experiments based on the BrainWeb phantom. PET-MR registration mismatches were additionally modeled. Imperfect segmentation was obtained by segmenting MR images with SPM12. Bias and coefficient of variability (COV) were computed for quantitative comparison. Results indicated PVC methods with subtle use of MR guidance to show stronger resilience to imperfect MR information compared to methods with stronger assumptions invoked in MR-guided PVC.

I. Introduction

POSITRON emission tomography (PET) is a powerful imaging tool which performs quantitative measurement of tracer concentrations. At the same time, quantitative accuracy of PET is degraded by partial volume effect (PVE) due to its limited spatial resolution. Different methods have been proposed for partial volume effect correction (PVC). High resolution MR images provide anatomical guidance that can be potentially used to improve the performance of PVC. Early methods such as geometric-transfer matrix (GTM) require segmentation of MR images into different regions and also make the strong assumption that activity distribution in each region is constant [1]. Though these methods have shown good performance when perfect guidance is available, mismatch between PET images and MR guidance may degrade performance of these methods.

Our hypothesis is that methods that make subtle usage of MRI images can prove more advantageous and depict greater feasibility and strength for translation to routine usage. Recently, we proposed anatomically-guided non-local means (NLMA) which makes usage of segmented MR images only to restrict the search space in non-local means framework without making any assumption for PET activity distributions in segmented MR regions [2], [3]. We also focus on the parallel level sets (PLS) framework, which has been developed for PET reconstruction in [4], while we push this method from its ordinary smooth optimization framework to a non-smooth optimization framework with some advantages. The Bowsher prior can also be considered as a method that makes subtle usage of MRI images. The latter two frameworks (PLS and Bowsher) are also potentially advantageous in that they do not require segmentation of MR images [4], [5], [6].

In this work, we compare different MR-guided post-reconstruction PVC methods. Specifically, we pursue our two recently proposed methods, namely NLMA and split Bregman based PLS (SBPLS) methods, as well as symmetric (sBowsher) and asymmetric Bowsher (aBowsher), and ordinary PLS solved with smooth optimization technique. We also include the region-based voxel-wise (RBV) method, a GTM-based method that works at the voxel level [7]. Reblurred Van Citter (VC) deconvolution method is also included as reference method which does not employ MR information at all [8]. These PVC methods are evaluated with both perfect and imperfect MR guidance due to mismatches in segmentation and registration.

II. Methods and Materials

A. PVC methods

The implementation of RBV and reblurred VC are described in [7], [8]. For other PVC methods, we describe with respect to the following regularized deconvolution problem:

$$\boldsymbol{f} = \arg\min_{\boldsymbol{f}} \|\boldsymbol{g} - \boldsymbol{h} * \boldsymbol{f}\|_2^2 + \lambda R(\boldsymbol{f}), \quad (1)$$

where $\boldsymbol{g}$ and $\boldsymbol{f}$ are uncorrected and corrected PET images, respectively, $\boldsymbol{h}$ denotes system point spread function (PSF),

Manuscript received December 18, 2019. This work was supported by NIH R21 grant AG056142, BC Cancer Foundation, and the Natural Science Foundation of Guangdong Province, grant 2018A030313366.

Yansong Zhu is with Department of Electrical and Computer Engineering, Department of Radiology and Radiological Science, Johns Hopkins University, USA, and Department of Radiology and Physics, University of British Columbia, Canada. (e-mail: yzhu46@jhu.edu)

Yuanyuan Gao is with the School of Biomedical Engineering, Southern Medical University, China.

Arman Rahmim is with Department of Radiology and Radiological Science, Johns Hopkins University, USA, and Department of Radiology and Physics, University of British Columbia, Canada.

978-1-7281-4164-0/19/$31.00

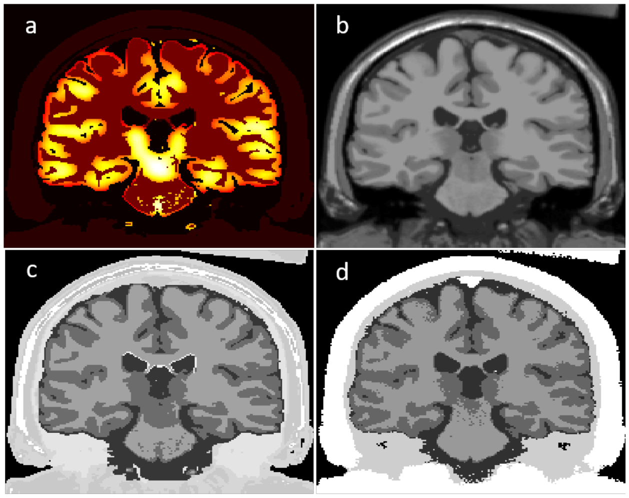

Fig. 1: (a) Simulated PET phantom. (b) MR image. (c) Tissue map with perfect segmentation. (d) Imperfect tissue map segmented with SPM12.

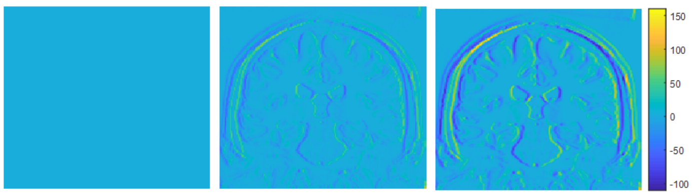

Fig. 2: Difference image between perfect MR guidance and imperfect MR guidance with registration mismatch ranging from 0 mm (left), 1 mm (middle) and 2 mm (right).

$R(\boldsymbol{f})$ is the particular MR-guided regularization, and λ denotes the regularization parameter. Regularization models for sBowsher, aBowsher, and PLS were described in [4], [5], [6]. The corresponding minimization problems were solved with limited-memory BFGS method. For our proposed SBPLS, we developed a non-smooth optimization technique based on split Bregman method to solve PLS regularization problem without adding a smoothness parameter [9]. The model of NLMA has been described in [2], [3]. Similar as [3], we solved the minimization problem using the Gauss-Seidel algorithm.

B. Experiments

Realistic PET simulation phantom was generated using the BrainWeb phantom [10]. The PET phantom was further processed to create non-uniform activity distributions in gray matter, as shown in Fig. 1(a). Realistic simulations were performed, setting system PSF to 4.5 mm and including Poisson noise in sinogram data, followed by OSEM reconstructions with 10 subsets and 24 iterations. Reconstructed images were then used as input for different PVC methods. Fig. 1(b) shows MR image directly used as guidance in segmentation-free methods. For RBV and NLMA, segmented tissue maps were provided as guidance. In order to study the influence of imperfect MR guidance, we simulated mismatches in segmentation and registration. For segmentation, we took both a perfect tissue map (referred to as perfect_seg) which is the same as the one we used to generate simulated PET phantom, and an imperfect tissue map (referred to as imperfect_seg)

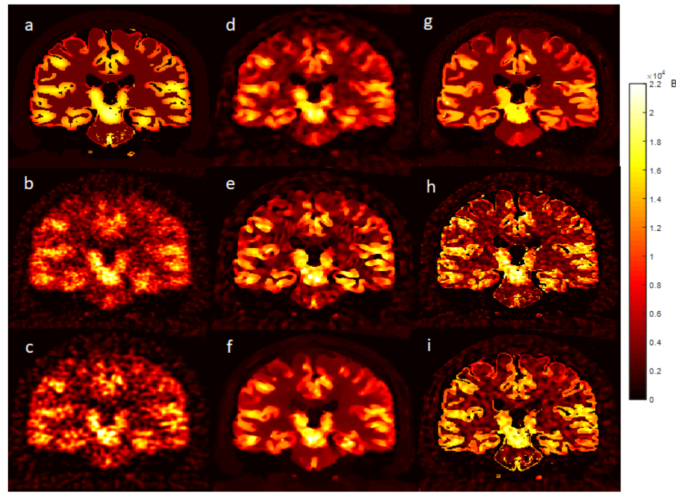

Fig. 3: Results of different PVC methods with perfect MR guidance. (a) Ground truth. (b) Uncorrected. (c) Reblurred VC. (d) sBowsher. (e) aBowsher. (f) smooth_PLS. (g) SBPLS. (h) RBV. (i) NLMA

obtained by segmenting the corresponding MR image with SPM12, as shown in Fig. 1(c) and Fig. 1(d). For registration, different extents of registration mismatches were simulated by shifting anatomical images. Fig. 2 shows difference image between perfect MR guidance and imperfect MR guidance with registration mismatch ranging from 0 to 2 mm. To evaluate quantitative performance of different PVC methods, mean percentage bias and coefficient of variability (COV) based on 20 noise realizations were computed. Bias-COV curves were obtained by changing regularization strength λ.

III. Results and Discussion

Fig. 3 depicts results of different PVC methods with perfect MR guidance (no errors in registration and segmentation). We observed all MR-guided PVC methods show improvements compared to uncorrected image and reblurred VC method. Among different MR-guided PVC methods, smooth PLS and sBowsher generated images with blurry edges, while other PVC methods were able to preserve sharp edges.

Fig. 4 shows bias-noise (COV) curves for these methods in gray matter and white matter when registration error ranges from 0 mm to 2 mm. With perfect segmentation and no registration mismatch, the two segmentation-based methods, RBV and NLMA show better performance compared to other methods. Amongst the segmentation-free methods, aBowsher and SBPLS outperformed sBowsher and PLS with smoothing, with SBPLS slightly outperforming aBowsher. With imperfect segmentation, performances of NLMA and RBV degraded. In this case, NLMA and RBV showed similar performance as SBPLS and aBowsher.

As registration mismatch increases, all MR-guided PVC methods degraded in performance. We observed in white matter, where uniform activity distribution was assigned in simulated PET phantom, performance of RBV was similar as NLMA for both perfect MR segmentation and imperfect MR segmentation. However, in gray matter, where non-uniform PET activity distribution was assigned, we notice faster degra-

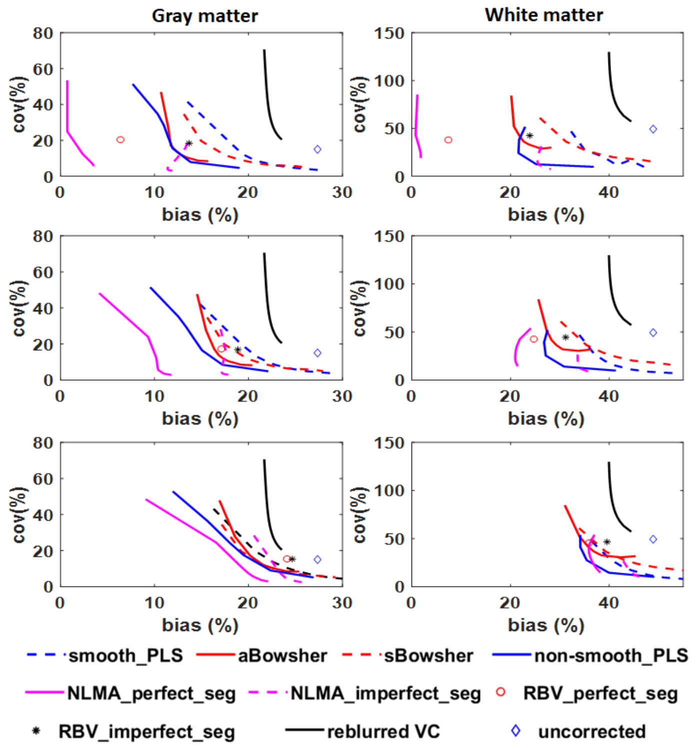

Fig. 4: Bias-noise trade-off curves for different PVC methods with registration error of 0 mm (top row), 1 mm (middle row) and 2 mm(bottom row) in gray matter (left column) and white matter (right column)

dation for RBV relative to other methods. With 2 mm registration mismatch, RBV shows similar performance to reblurred VC even with perfect MR segmentation. In contrast, NLMA shows stronger resilience to segmentation and registration mismatches. We observed NLMA with perfect segmentation provided best performance in most cases, except for the case of 2 mm registration mismatch in white matter, where its performance is similar as SBPLS and aBowsher. When imperfect MR segmentation was provided, performance of NLMA was inferior compared to SBPLS and aBowsher in most cases. This indicates that good segmentation is still essential to guarantee the performance of NLMA. Among different segmentation-free methods, our proposed SBPLS showed best performance in all registration mismatch cases. We also experimented with larger (3 mm and beyond) registration mismatches (not shown here), and differences between different methods with subtle MR guidance were no longer obvious, but they all performed better than RBV.

IV. Conclusion

We compared different MR-based PVC methods in the context of varying MR information mismatches. We showed that PVC methods with subtle MR guidance, including our proposed methods, demonstrate stronger resilience to mismatches between PET and MR images compared to methods with stronger assumptions invoked in MR-guided PVC.

References

[1] O. G. Rousset, Y. Ma, and A. C. Evans, “Correction for partial volume effects in pet: principle and validation,” *Journal of Nuclear Medicine*, vol. 39, no. 5, pp. 904–911, 1998.

[2] Y. Gao, M. Bilgel, S. Ashrafinia, L. Lu, O. Rousset, S. Resnick, D. Wong, and A. Rahmim, “Evaluation of non-local methods with and without anatomy information for improved quantitative amyloid pet imaging,” *Journal of Nuclear Medicine*, vol. 59, no. supplement 1, pp. 1779–1779, 2018.

[3] Y. Gao, H. Zhang, Y. Zhu, M. Bilgel, O. Rousset, S. Resnick, D. F. Wong, L. Lu, and A. Rahmim, “Voxel-based partial volume correction of amyloid pet images incorporating non-local means regularization,” in *2018 IEEE Nuclear Science Symposium and Medical Imaging Conference Proceedings (NSS/MIC)*. IEEE, 2018, pp. 1–4.

[4] M. J. Ehrhardt, P. Markiewicz, M. Liljeroth, A. Barnes, V. Kolehmainen, J. S. Duncan, L. Pizarro, D. Atkinson, B. F. Hutton, S. Ourselin *et al.*, “Pet reconstruction with an anatomical mri prior using parallel level sets,” *IEEE transactions on medical imaging*, vol. 35, no. 9, pp. 2189–2199, 2016.

[5] J. E. Bowsher, H. Yuan, L. W. Hedlund, T. G. Turkington, G. Akabani, A. Badea, W. C. Kurylo, C. T. Wheeler, G. P. Cofer, M. W. Dewhirst *et al.*, “Utilizing mri information to estimate f18-fdg distributions in rat flank tumors,” in *IEEE Symposium Conference Record Nuclear Science 2004.*, vol. 4. IEEE, 2004, pp. 2488–2492.

[6] K. Vunckx and J. Nuyts, “Heuristic modification of an anatomical markov prior improves its performance,” in *IEEE Nuclear Science Symposuim & Medical Imaging Conference*. IEEE, 2010, pp. 3262–3266.

[7] B. A. Thomas, K. Erlandsson, M. Modat, L. Thurfjell, R. Vandenberghe, S. Ourselin, and B. F. Hutton, “The importance of appropriate partial volume correction for pet quantification in alzheimers disease,” *European journal of nuclear medicine and molecular imaging*, vol. 38, no. 6, pp. 1104–1119, 2011.

[8] J. Tohka and A. Reilhac, “Deconvolution-based partial volume correction in raclopride-pet and monte carlo comparison to mr-based method,” *Neuroimage*, vol. 39, no. 4, pp. 1570–1584, 2008.

[9] T. Goldstein and S. Osher, “The split bregman method for l1-regularized problems,” *SIAM journal on imaging sciences*, vol. 2, no. 2, pp. 323–343, 2009.

[10] C. A. Cocosco, V. Kollokian, R. K.-S. Kwan, G. B. Pike, and A. C. Evans, “Brainweb: Online interface to a 3d mri simulated brain database,” *NeuroImage*, vol. 5, p. 425, 1997.